GREEN SYNTHESIS OF Ag NANOPARTICLES ON REDUCED GRAPHENE OXIDE NANOCOMPOSITE AND PROMISING APPLICATION FOR METHYLENE BLUE DYE REMOVAL

JOSEPHINE SARAH STEPHENSON[1], BALAMURUGAN ARUMUGAM[2], SAYEE KANNAN RAMARAJ[2*]
Department of chemistry,Infant Jesus college of Engineering, Thoothukudi-51[1]
Department of chemistry, Thiagarajar College, Madurai-09[2*].

Abstract

A facile green process was developed for the synthesis of AgNPs - rGO composite by using *Citrullus colocynthis* leaf extract as a reducing and stabilizing agent. The morphology and microstructure of the magnetic nanocomposite was examined by FTIR, XRD, UV-VISIBLE and SEM. Here, the green synthesized nanocomposite display remarkable effective removal of Methylene Blue (MB) from aqueous solution, showing a maximum adsorption capacity reached up to 146.43 mg g-1 within only 30 mints at room temperature. The kinetics, isotherms and thermodynamics of the adsorption of MB have been studied at various experimental conditions (initial dye concentration of MB, adsorbent dosage, contact time and temperature). Adsorption kinetics and the equilibrium adsorption isotherm were found to follow a pseudo-second order kinetic model and Langmuir isotherm, respectively. The thermodynamic parameters indicated that the adsorption was spontaneous, favorable, and endothermic in nature. Moreover, AgNPs - rGO was very stable and can be readily reuse by washing with water. Therefore we believed that the prepared nanocomposite as a very good green adsorbent for eliminating MB from aqueous solution.

Key words: AgNPs- rGO composite, Methylene blue, Adsorption

1.INTRODUCTION

Nowadays, metal nanoparticles are gaining great interest in treatment of pollutants contaminated waste water. Particularly, Silver nanoparticles (AgNPs) have many promising applications in nanotechnology because of their good electrical conductivity, chemical stability, catalytic and antibacterial properties.[1] These properties depend mainly on their size, shape, composition, structure and morphologies[2]. biosensors[3], catalysts [4], and environment remediation [5]. Due to large specific surface area, high surface reactivity [6], high affinity [7] and low cost, AgNPs are promising adsorbent for environmental applications. It can be synthesized by various methods such as, vacuum sputtering [8], decomposition in organic solvents [9] and chemical reduction with sodium borohydride($NaBH_4$)[10]. Generally, AgNPs produced by chemical reduction of Silver with $NaBH_4$ as a reducing agent is a routine synthesis reported so far. Stabilizers such as chitosan [11], activated carbon [12] and carboxymethyl cellulose [13] are commonly added in these reduction methods to synthesize stable, small size AgNPs. Among, these syntheses are generally expensive and require special equipment, high energy and involve chemical substances that are toxic, costly, corrosive and flammable, and non eco-friendly [14].To conquer this problem, nowadays a simple, cost effective and environmentally friendly new green reduction method being preferred. Compare to the other biological systems the plant materials make attractive platform for bioreduction due to low cost cultivation, short production time, safety and the ability to large scale production of AgNPs. Moreover, homogeneous AgNPs is undesirable for industrial and environmental application because of their number of drawbacks such as easy oxidation, rapid agglomeration, difficult in solid/liquid separation and adsorbent recycling become major challenges. In order to overcome these challenges, metal nanoparticles(MNPs) are generally anchored on sand [15], zeolite [16], clay[17] and carbon[18]. Considering safety and efficiency, Carbon-based nanomaterials including activated carbon[19], graphene [20] and carbon nanotubes [21] have widely been used as supporters for MNPs. One of the major advantages of carbon-based nanoparticles as attractive adsorbents is that they have much larger specific surface areas which improve the dispersibility of MNPs than many other materials. Recent developments in the use of graphene oxide (GO) showed immense promise in its application for separation and detection of trace levels of organic and inorganic analytes [22]. Generally, Graphene supported AgNPs are emerging adsorption materials because of its sheet structure, associated band structure [23], high specific surface area, extended conjugation of pi-electron [24], dispensability in water and low cost [25]. Therefore, it

is reasonable to believe that graphene-based NPs composites can be used as promising adsorbent for practical applications in environmental toxic pollutants to benign form.

Synthetic dyes used in a wide range of industries such as textile, leather, paper, printing, and other industries are often intended to be able to resist the breakdown of long-term exposure to sunlight, water and other conditions, which makes the treatment of the dye wastewater more difficult [26]. Particularly, Methylene Blue (MB) was well-known cationic dyes, which have been widely used in textile, printing, and research laboratories. MB was widely investigated toxic pollutants in industrial wastewater and could cause a wide range of health problems. On inhalation of MB, can give rise to short periods of rapid or tricky breathing, while ingestion through the mouth produces a burning sensation and may cause nausea, vomiting, diarrhea, and gastritis. A large amount creates abdominal and chest pain, severe headache, profuse sweating, mental confusion, painful micturation, and methemoglobinemia-like syndromes [27]. Drinking water containing these pollutants could cause serious disorders, such as cancer and mental retardation [28]. Efficient decolorization treatment of dyes has therefore received great attention. Among many chemical, physical, and biological treatment of pollutant removal such as, degradation [29], separation [30], electrochemical treatment [31], coagulation [32], filtration [33], flotation [34], softening, ion exchange [35], catalytic reduction [36] and chemical oxidation [37]. Among all these methods technical and economical feasibility problem. On the other hand adsorption is one of the most effective methods for MB removal because of its low cost, high efficiency, simplicity and insensitivity to toxic substances [38].

In this present work a green synthesized AgNPs-rGO composites by *Citrullus colocynthis* leaf extract as both reducing and capping agent. The obtained material was characterized by UV, FT-IR, XRD and SEM analysis. The decolorization efficiency of green synthesized AgNPs-rGO composites is examined by using MB dye. To the best of our knowledge, this is the first study that reports on green synthesized AgNPs-rGO composites for scavenger of wastewater pollutants. The formation and adsorption mechanism of AgNPs-rGO are investigated and discussed. The effects of contact time, initial dye concentrations, temperature and adsorbent mass on the adsorption process were also discussed.

2. MATERIALS AND METHODS

2.1. Materials

Natural graphite powder, Methylene blue (MB) [$C_{16}H_{18}N_3OS$, MW: 333.6 g mol^{-1}, λ_{max}: 630 nm], sulfuric acid (H_2SO_4, 98%), hydrochloric acid (HCl, 37%), hydrogen peroxide (H_2O_2), sodium nitrate ($NaNO_3$), potassium permanganate, ($KMnO_4$), Silver Nitrate($AgNO_3$), were purchased from Sigma-Aldrich, India. *Citrullus colocynthis* leaf was collected from local area in Madurai, Tamil Nadu. All aqueous solutions used in this work were prepared by deionized water. All chemicals are analytical purity and were used without any further purification.

2.2. Synthesis of GO

Graphene oxide (GO) was synthesized from natural graphite powder by a modified Hummers method [39]. Briefly, 1g of graphite powder was added to the mixture of 0.5g of $NaNO_3$ and 25 mL H_2SO_4 into a 250 mL beaker following by 30 min stirring at 0^0C. Subsequently, 6 g of $KMnO_4$was added slowly to the suspension with stirring. After stirring for 2 h, the temperature of the mixture was heated to $35^0C \pm 5^0$C for 30 min. 90 mL of water was slowly added and then the solution was further heated to 90 ^{0}C under vigorous stirring for 15 min. Then, 60 mL of H_2O_2 aqueous solution was added to the suspension until its color was changed from drab to brilliant yellow to reduce the residual MnO_2. The yellow graphite oxides were washed by diluted HCl (5%) and DI water three times to eliminate SO_4^{2-} and H^+ respectively. Finally, the resulting solid was dried in a vacuum oven at 50 ^{0}C for 24 h to get GO.

2.3. Preparation of aqueous *Citrullus colocynthis* leaf extracts (CCLE)

Locally collected fresh *Citrullus Colocynthis* leaves were cleaned. The aqueous extract was prepared by the addition of 20g of leaves with 100 ml distilled water at 80^0C for 5min. Further the extract was filtered and the filtrate was stored (10^0C) for further use.

2.4. Synthesis AgNPs-rGO composite

AgNPs-rGO composites were synthesized by green method. The synthesis methods of AgNPs-rGO composite were carried out as follows: $AgNO_3$ (in 50ml) solution was mixed into the GO aqueous solution (10ml, 0.1mg/1ml). The mixture was magnetically stirred for 10 mints to form homogeneous solution. Then, 60ml of freshly prepared aqueous CCLE was added drop wise into the above solution followed by further stirring for 30 min at 60^0C. The resulting suspension was centrifuged for 10 min and washed with water for several times to get free of excess chemicals. Finally the residue was dried at 50^0C to yield AgNPs-rGO composites. Similar procedures were used to synthesize of AgNPs was also carried out without GO using the same experimental conditions.

2.5. Preparation of Stock Solution

The MB stock solution of 500 ppm concentration was prepared by dissolving an accurately weighted amount of MB in DI water. The desired concentrations of the solution were obtained by diluting the stock of MB solution in exact proportions to obtain different initial concentrations.

2.6. Adsorption Experiments

Adsorption of MB onto the AgNPs-rGO composite was investigated by a batch method. Batch adsorption experiments have been performed by mixing 50mL of a dye solution (250 ppm to 500 ppm of concentration) with 5 mg to 30 mg of the AgNPs-rGO composite in 250 ml iodine flask at stirring rate 120 rpm. Sample flasks were shaken on a shaker and operated at a constant temperature of 35^0C and 120 rpm for 1 h. Finally, 5mL of sample was continuously taken for adsorption analysis at appropriate time intervals (0, 6, 12, 18, 24, 30 and 60 min) and the adsorbed amount of dyes was calculated by Beer's law. Then, dye solutions were separated from the mixture by centrifuge (12000 rpm for 20 min) and analyzed by UV−vis spectroscopy. Concentration of the dye solution was determined colorimeterically by measuring at maximum absorbance of the MB dye (λ_{max} = 663 nm). Preliminary experiments indicated that the adsorption of MB reached equilibrium in 30 mints. Thus, the contact time of 1h was selected in the batch experiments. The adsorption capacity of AgNPs-rGO composite was determined by using the following equation

$$q_e = (C_o - C_e)V/m \quad (1)$$

Where C_o is the initial concentration of MB (ppm), C_e is the concentration of MB at equlibirium (ppm), V is the total volume of the suspension (L), and m is the mass of adsorbent (g).

Kinetic studies were performed at a constant temperature of 35 °C and 120 rpm with 500 ppm of initial concentration of dye solutions at a predetermined time interval ranged from 0 to 60 min. The amount of adsorbed dye on adsorbents (q_t, mg/g) was calculated as follows

$$q_t = (C_o - C_t)V/m \quad (2)$$

Where C_o is the initial concentration of MB (ppm), C_t is the concentration of MB at time t (ppm), V is the total volume of the suspension (L), and m is the mass of adsorbent (g).

The thermodynamic studies of MB onto the AgNPs-rGO composite was carried at four different temperatures namely 25, 35 and 40 ^{0}C in aqueous medium.

2.7. Adsorption isotherm.

In a typical batch adsorption isotherm experiments were carried out at 30 mg of AgNPs-rGO composite was mixed with 50 mL of solution of different initial concentrations at room temperature, with no other additives present, and stirred for 1h to ensure adsorption equilibrium.

2.8. Characterization.

. The samples were applied to 300 mesh copper grids with lacey supported film. The crystallographic structure of the materials was studied by a powder X-ray diffraction (XRD) (Panalytical X' per PRO X-ray diffractometer) equipped with Cu Kα radiation (λ = 0.15406 nm). UV−vis detection was carried out on a UV-1800 SHIMADZU spectrophotometer. Fourier transform infrared (FTIR) spectra were recorded by a Shimadzu model FT-IR spectrometer. The structural morphology of the AgNPs-rGO composite was studied by SEM imaging.

3. RESULTS AND DISCUSSION

FT-IR Spectroscopy

The functional groups present in the GO and AgNPs-rGO represented by FT-IR Spectroscopy.

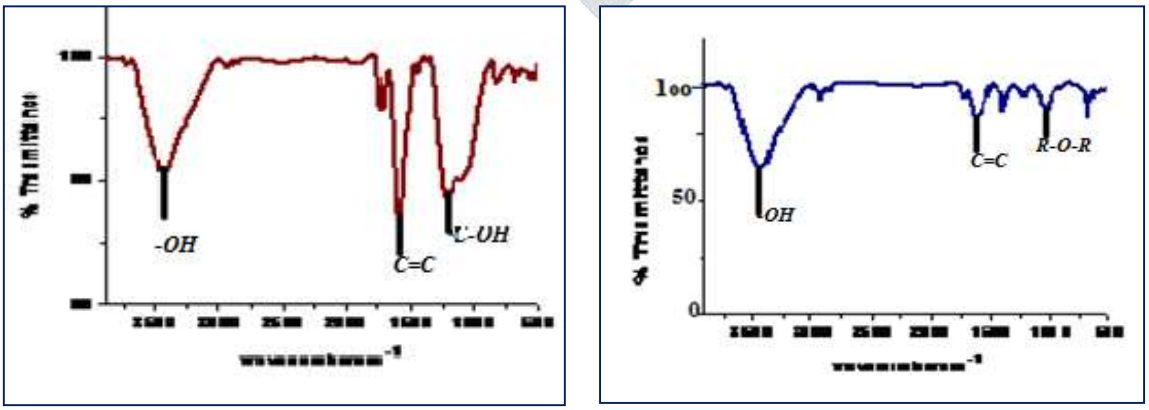

fig.5.2. ft-ir spectra of (a) GO and (b) AgNPs-rGO

The absorption peak at 1620 cm^{-1} can be ascribed to the skeletal vibrations of unoxidized graphitic domains (C=C) or contribution from the stretching deformation vibration of intercalated water[23,24]. In addition, the C-OH stretching peak at 1220 cm^{-1} and C=O stretching peak attributed to epoxy or alkoxy at 1060 cm^{-1} can also be observed. After adding leaf extract, during preparation of AgNPs-rGO composite, the C=O vibration band disappears, and the broad O-H and the C=O stretching bands remain. As the adsorption bands of oxygen functionalities disappear (C=O groups are considerably decreased) and only the peak at 1620 cm^{-1} remains, it demonstrates that rGO is achieved by addition of leaf extract during the preparation of AgNPs-rGO composite..

XRD

The XRD patterns as shown in (Fig.2.a) were performed to analyze the crystalline structure. Comparison of the micrograph shows that before and after adsorption of metal ion on the surface of the material. The XRD data provided evidence of decrease in the peak intensity of 2θ values which shows that adsorption of metal ions on the surface of the adsorbent (Fig.2.b) indicate that decrease in the peak intensity values after adsorption of MB on the surface of the material.

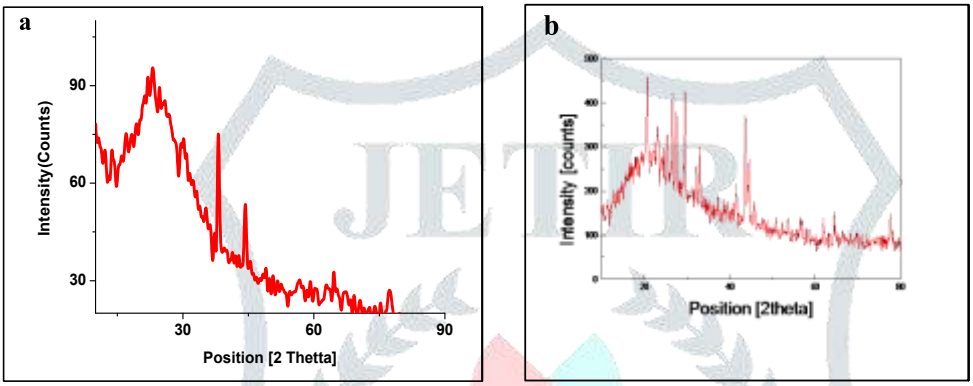

fig.2: a and b xrd pattern of AgNPs-rGO before adsorption and after adsorption

ADSORPTION ISOTHERM

To investigate the nature of interaction of AgNPs-rGO composite, rGO and AgNPs with MB dye molecule, adsorption isotherms experiments at different experimental conditions were carried out. The adsorption characteristics at equilibrium were analyzed by using Langmuir [42] and Freundlich [43] models and presented in Fig.3 & 4. Based on the adsorption data of the specimens shown in Table 1, the correlation coefficients of the isotherms are relatively high (0.997 for AgNPs-rGO composite, 0.990 for rGO and 0.983 for AgNPs) which shows that the Langmuir isotherm model is better fit for describing the adsorption equilibrium of MB onto AgNPs-rGO composite, rGO and AgNPs with than Freundlich isotherm model. From that, the monolayer adsorption on structurally and energetically homogeneous active sites and predicts the monolayer coverage at the outer surface of the adsorbent [42].

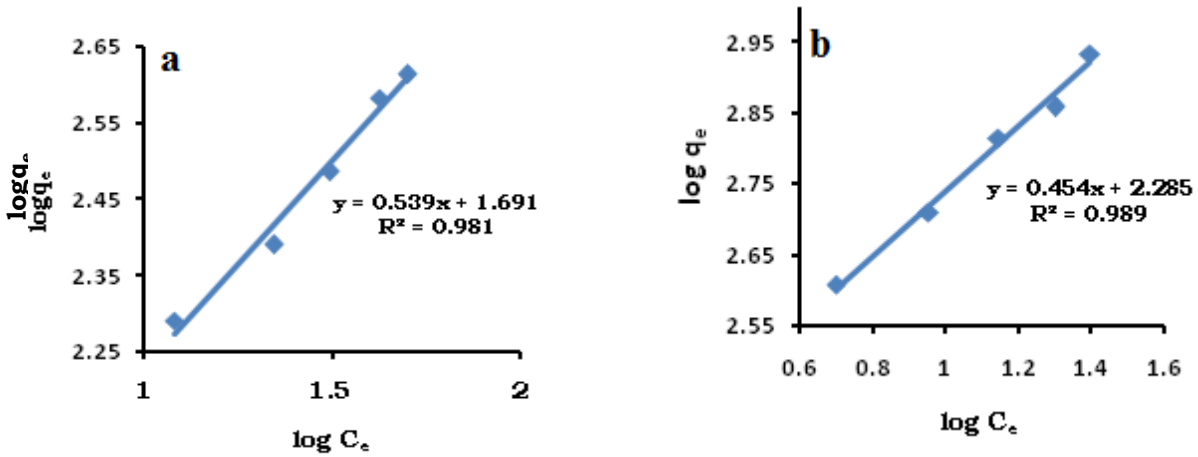

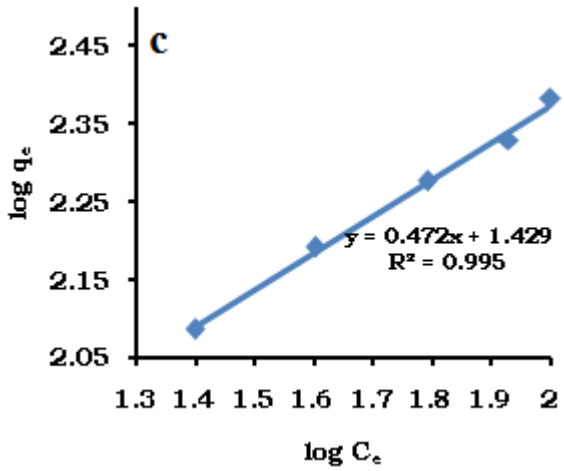

fig.3. freundlich adsorption isotherm for the adsorption of MB by a) rGO b) AgNPs c) AgNPs-rGO

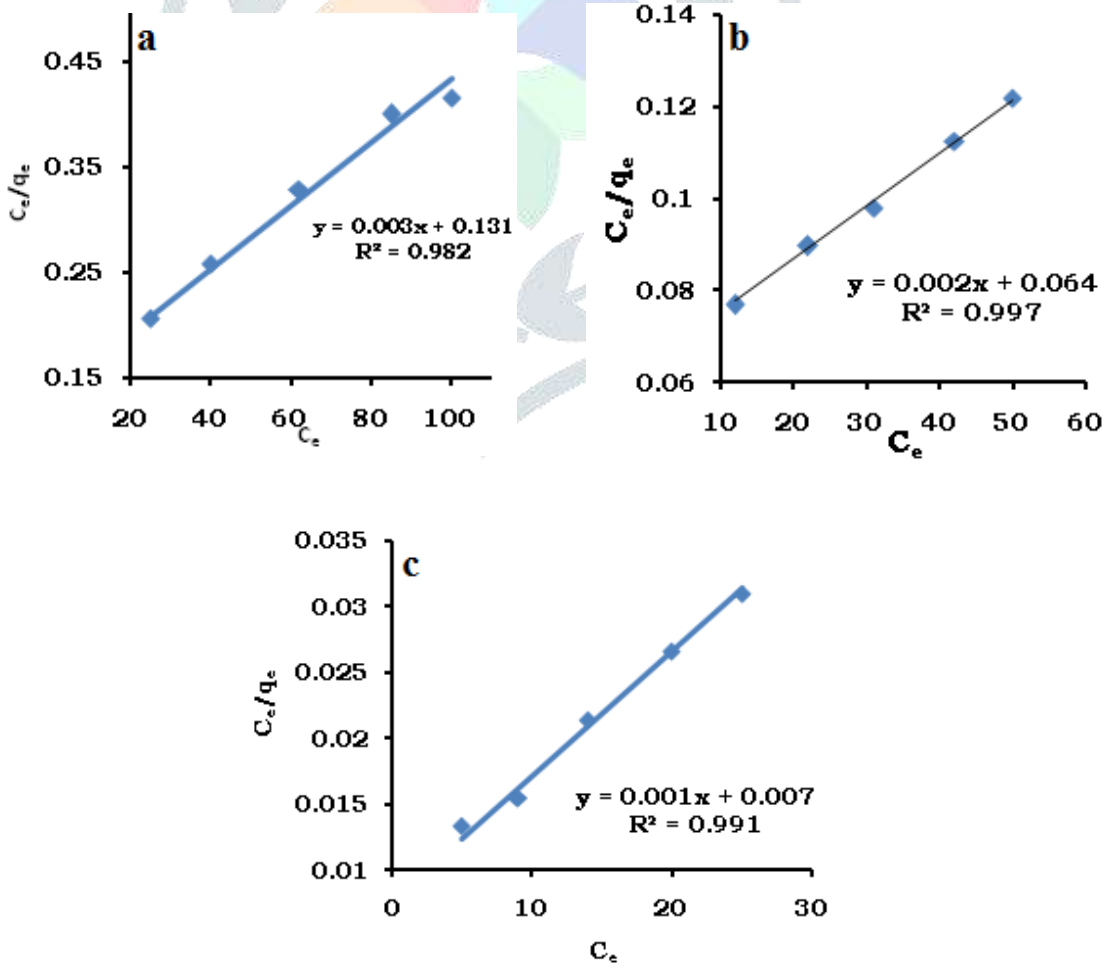

fig.4. langmuirs adsorption isotherm for the adsorption of MB by a) rGO b) AgNPs c) AgNPs-rGO

The R_L value indicates the shape of the isotherm to be either unfavorable (R_L> 1), linear (R_L= 1), favorable (0<R_L<1), or irreversible (R_L= 0). In the present investigation the R_L was found to be 0.0223, 0.0609 and 0.183 for AgNPs-rGO composite, rGO and AgNPs respectively indicating that the adsorption of MB is favorable.

table.1. adsorption isotherm parameters for the adsorption of MB

	Langmuir				Freundlich		
Adsorbent	K_L (1/mg)	q_m (mg/g)	R_L	R^2	K_F	1/n	R^2
AgNPs-rGO	0.163	877.19	0.007	0.991	192.75	0.225	0.995
AgNPs	0.031	500.00	0.0609	0.997	49.091	0.156	0.989
rGO	0.023	333.33	0.116	0.982	26.853	0.008	0.981

Adsorption Kinetics

The adsorption Kinetics models were applied to investigate the adsorption rate and detailed mechanism of adsorption process. In general, the adsorption rate is considered as one of the most important factors for choosing an ideal adsorbent [44].To study the adsorption mechanism well, pseudo first-order and pseudo second-order equations were used to applied. The Lagergren pseudo first-order kinetic model is expressed as [45]

$$\log (q_e - q_t) = \log q_e - k_1 t/2.303 \quad (3)$$

Ho and McKay pseudo-second order kinetic model is expressed as [46]

$$t/q_t = 1/k_2 q_e^2 + t/q_e \quad (4)$$

where, q_e and q_t are the adsorption capacity of MB onto the synthesized material at equilibrium and at time t, respectively. k_1 (min^{-1}) and k_2 (g/mg.min) also represent the rate constant of pseudo-first-order and pseudo-second-order kinetic models, respectively. The estimation of two models was performed by plotting the values of log (q_e-q_t) Vs t for pseudo-first-order model (fig. 6.), t/q_t Vs t (fig. 5.) for pseudo-second-order model.

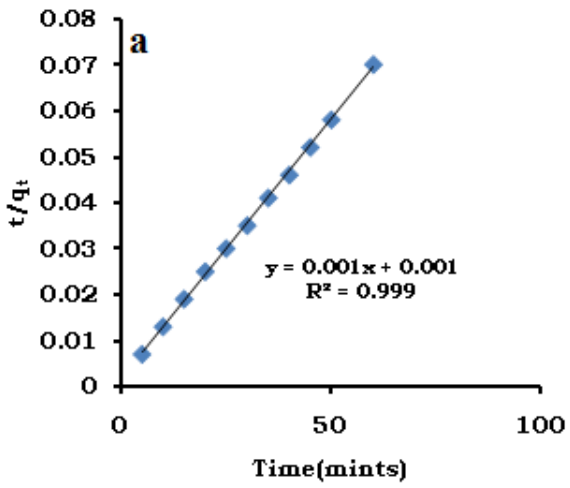

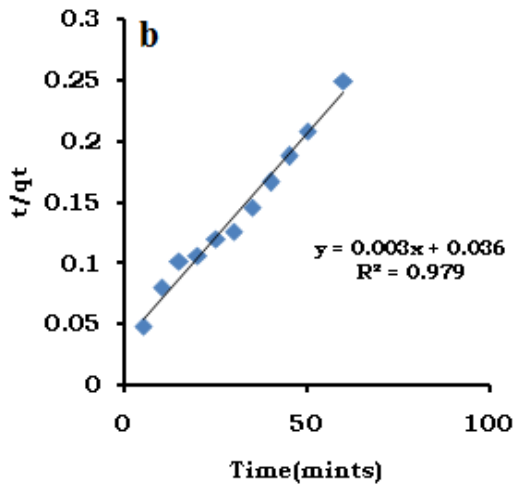

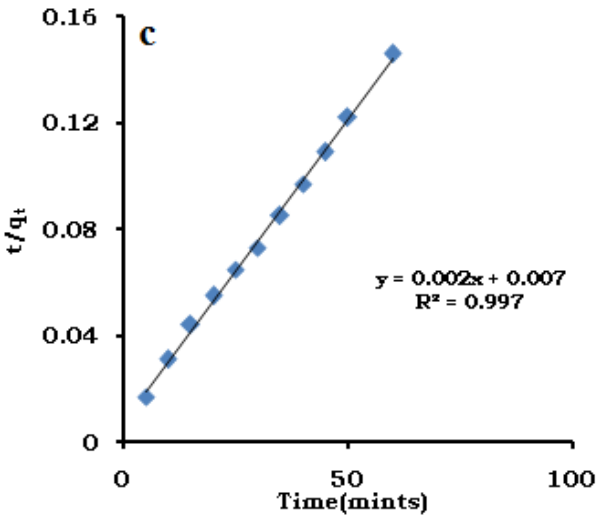

fig.5. pseudo second order kinetics plot for the adsorption of MB by a) rGO b) AgNPs c) AgNPs-rGO

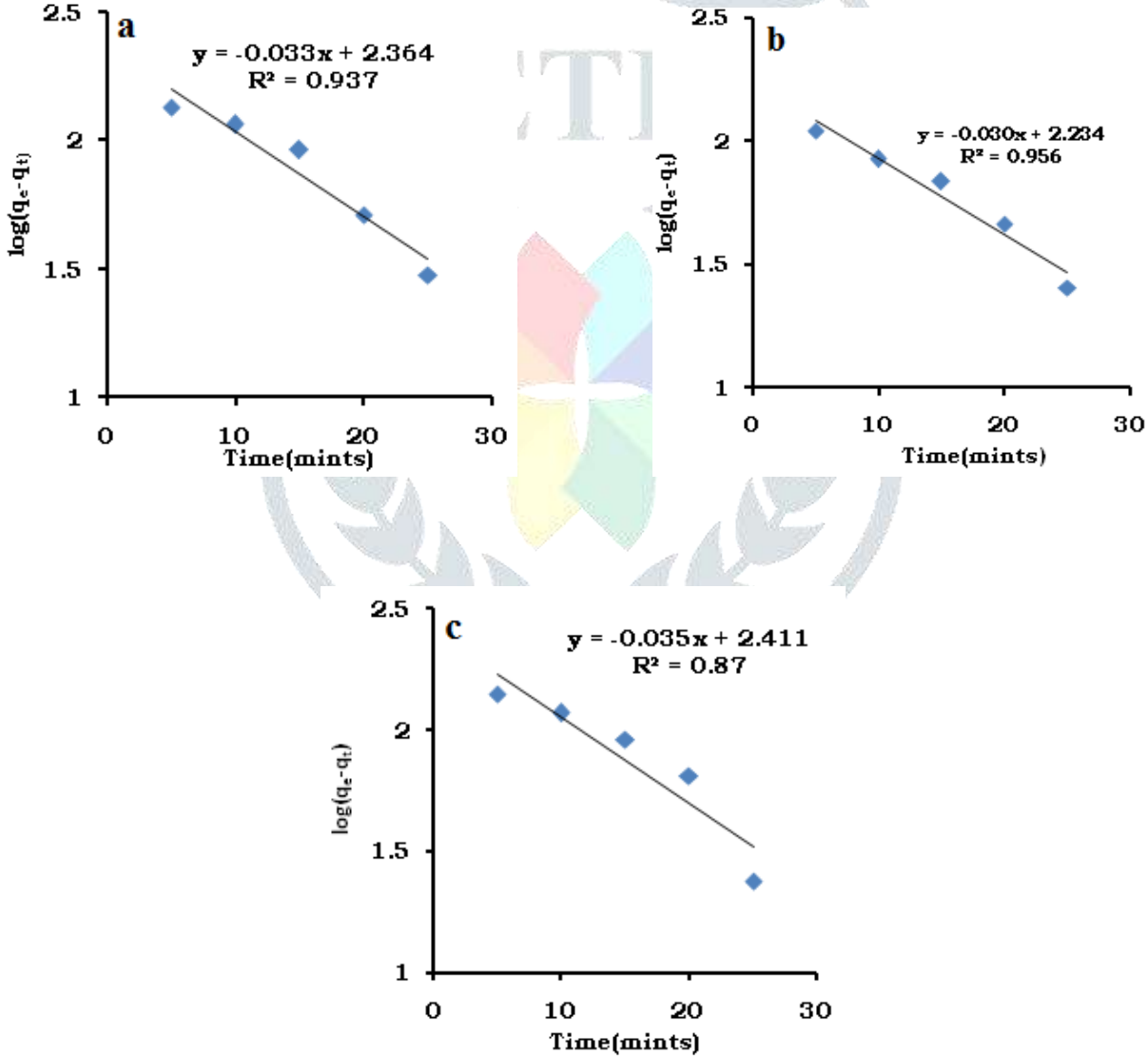

fig.6. pseudo first order kinetics plot for the adsorption of MB by a) rGO b) AgNPs c) AgNPs-rGO

The rate constants and qe were obtained from the slopes and intercept of corresponding plots. All the corresponding kinetics parameters are listed in Table 2. According to our results the adsorption of dyes are best evaluated by pseudo-second-order kinetic model due to high correlation coefficient.

Table.2. Adsorption Kinetic Parameters for the adsorption of MB

Adsorbent	q_e exp (mg/g)	Pseudo-first order model			Pseudo-first order model			Weber-Morris model		
		k_1 (min^{-1})	q_e cal (mg/g)	R^2	k_2 (min^{-1})	q_e cal (mg/g)	R^2	K_i (g mg^{-1} $min^{-0.5}$)	C (mg/g)	R^2
AgNPs-rGO	860.4	0.0806	257.632	0.87	0.001	1000.00	0.999	29.22	666.2	0.863
AgNPs	410.7	0.069	171.396	0.956	0.00057	500.00	0.997	22.31	263.1	0.876
rGO	240.6	0.076	231.3	0.937	0.00025	333.33	0.979	28.31	52.84	0.861

In addition, the calculated q_e values for pseudo-second-order kinetic model were best compliance with experimental q_e values thus also indicates that the overall rate of dyes adsorption processes follows pseudo second-order reaction mechanism. Since adsorption mechanism depends on the adsorbate and the adsorbent. Finally, the limiting rate in the adsorption of MB is a chemisorption mechanism through electrostatic attraction between active sites of adsorbent and dye molecules [47].

Intra particle diffusion model

It is vital to identify the steps involved during a solid liquid adsorption process. The adsorption process in porous solids could be described by three steps:(1) external mass transport of adsorbate from the bulk solution across the liquid film to the exterior surface of adsorbent (film diffusion or boundary layer diffusion or outer diffusion); (2) transport of adsorbate from the exterior surface of adsorbent to the pores or capillaries of the adsorbent internal structure, (intraparticle diffusion or inner diffusion);(3) the adsorption of adsorbed onto the active sites of adsorbent in inner and outer surfaces. Generally, the rate of adsorption is controlled by boundary layer diffusion or intraparticle diffusion or both. To find out the actual rate controlling step involved in the MB adsorption process, we applied the Weber−Morris equation. Plots of q_t Vs $t^{1/2}$ are shown in Fig.7 , and the corresponding kinetic parameters are listed in Table 2. The intra-particle diffusion constant and the boundary layer thickness were calculated using the linear equation [48].

$$q_t = k_{id}\, t^{1/2} + C \qquad (5)$$

where q_t is the amount of dye adsorbed onto the adsorbent at time t (mg/g), C is the boundary layer thickness, and k_{id} is the intra-particle diffusion rate constant(mg /g$min^{1/2}$)

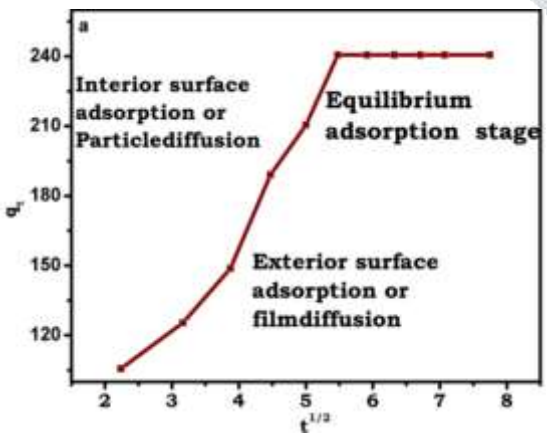

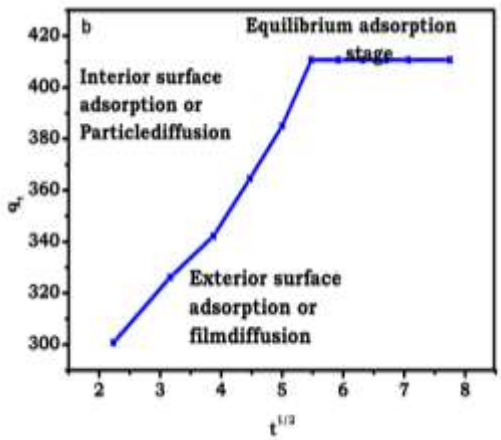

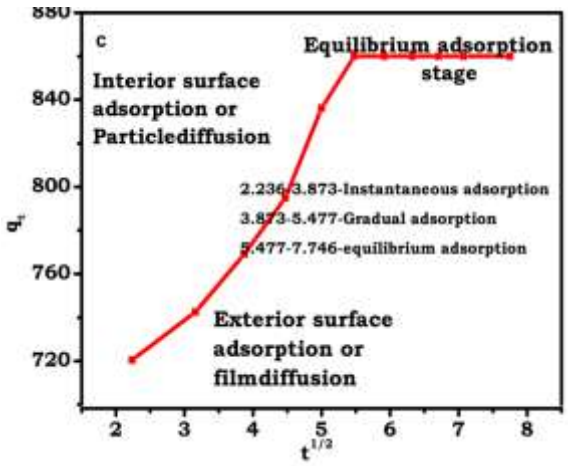

fig.7.webber - morris plot for intraparticle diffusion a) rGO b) AgNPs c) AgNPs-rGO

It was also examined that the plots are not linear over the whole time range which means that the intraparticle diffusion is not the rate determining step the overall adsorption process may be jointly controlled by external mass transfer and intraparticle diffusion, and intraparticle diffusion played a predominant role in controlling the adsorption mechanism of the model dye onto [49]. The divergence of the plot from the linearity suggesting that the rate-limiting step must be controlled boundary layer diffusion because of the large intercepts of linear portion of the plots. The larger intercept the greater is the boundary layer effect and this means that the adsorption is more boundary layer controlled [50]. As can be observed from the Fig.7 the regression of q_t versus $t^{1/2}$ have multi-linear portions which indicates that the three stages control the adsorption process. The instantaneous adsorption was occurred in the initial linear portion resulting from the diffusion of dye through the solution to the external surface of adsorbent. The gradual adsorption stage was occurred in second linear portion, corresponding to intraparticle diffusion of dye molecules through the pores of adsorbent. The equilibrium adsorption was occurred in the third stage where the intraparticle diffusion starts to slow down due to the extremely low adsorbate left in aqueous solution and the decrease of adsorption sites [51]

Adsorption thermodynamics

To get the information about the inherent energy change of adsorbent after adsorption and the mechanism of the adsorption process adsorption thermodynamics can be used. The thermodynamic parameters namely, the free energy change (ΔG° kJ/mol), enthalpy change (ΔH°, kJ/mol), and entropy change (ΔS°, kJ/mol K) of the adsorption of MB onto the rGO, and AgNPs, AgNPs-rGO were determined by using the following equations [44].

$$K_d = q_e/C_e \quad (6)$$

$$\Delta G^o = -RT \ln K_d \quad (7)$$

$$\ln K_d = \Delta S^o/R - \Delta H^o/RT \quad (8)$$

Where K_d is the distribution coefficient, T is the temperature (K), and R is the gas constant (8.314 J/mol K), respectively. ΔH° and ΔS° are obtained from the slope and intercept of van't Hoff plots of $\ln K_d$ versus T^{-1} (fig.8).

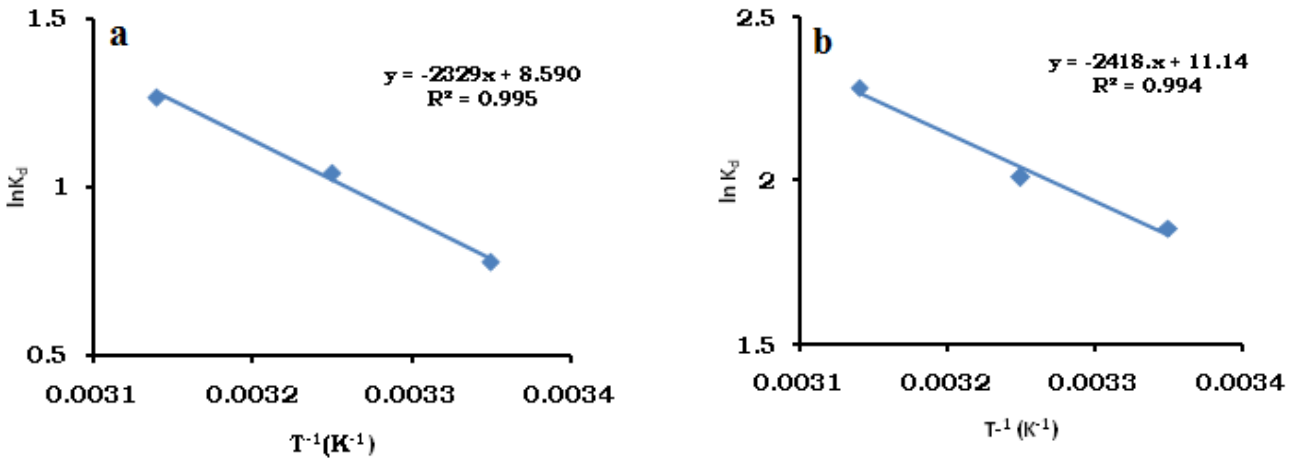

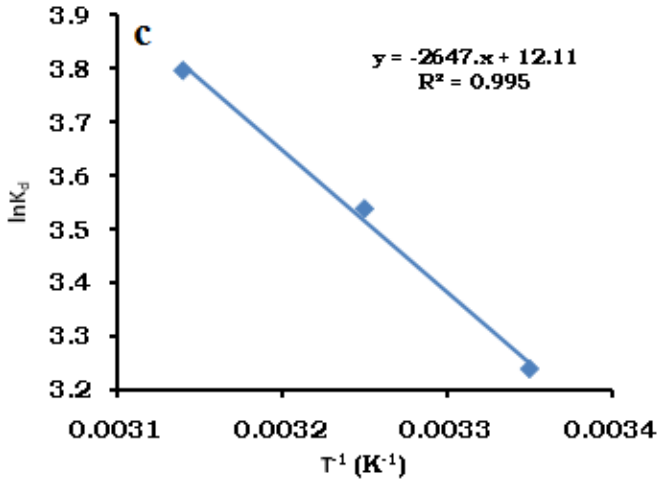

fig.8. van't koff plot of MB on rGO, AgNPs and AgNPS-rGO for calculation of thermodynamic parameters

The calculated ΔG^o, ΔH^o and ΔS° of the MB on rGO, AgNPs and AgNPs-rGO are given in Table.3. The negative values of ΔG° at difAgrent temperature indicate that spontaneous nature of MB adsorption on rGO, AgNPs and AgNPs-rGO. Generally the value of ΔG° for physisorption (−20 to 0 kJ/mol) is lesser than that of chemisorption (−80 to −400 kJ/mol) [52]. Therefore, the ΔG° results suggest that physisorption might dominate the adsorption of MB onto all the three system. It is also observed that the ΔG° value increases with increasing temperature of the adsorption system which indicates the more adsorption of the MB dye molecule onto the rGO, AgNPs and AgNPs-rGO surfaces. The positive values of ΔH°(22.0 for AgNPs-rGO, 20.1 for AgNPs and 19.36 for rGO) further confirm that the adsorption processes are endothermic in nature. The adsorption process is governed by physical adsorption process if the ΔH° is within the range of (1 to 93) $kJ \cdot mol^{-1}$ [53].

table. 3. thermodynamic parameters for the adsorption of MB

Adsorbent	ΔG^o(kJ/mol)			ΔH^o(kJ/mol)	ΔS^o(J/mol.K)
Temperature(K)	298	308	318		
rGO	-8.02	-9.06	-10.00	19.36	100.68
AgNPs	-4.59	-5.15	-6.04	20.10	92.62
AgNPs-rGO	-1.93	-2.66	-3.67	22.007	71.42

The ΔH° values for all the three systems are positive in the temperature range (298 to 318K) indicates the endothermic nature of adsorption [54]. Adsorption in the liquid phase is a complex phenomenon in which solute adsorbate and solvent compete for the solid adsorbent surface[53]. In the present system, the MB and water molecules compete for solid rGO, AgNPs and AgNPs-rGO and also the energetic changes involved in this process resulting positive ΔH°. The positive value of ΔS° indicates good affinity of MB dye toward the system and an increase in randomness at the solid−solution interface during the adsorption of MB on the active sites of rGO, AgNPs and AgNPs-rGO [54].

Adsorption mechanism

Nowadays, AgNPs have great attention in the degradation of contaminants due to strong reductive and attractive property. It is expected that the existence of rGO in the nanocomposite could improve the tendency of composite to remove the dye molecules. In this work, we use AgNPs-rGO composite to remove the MB molecules from aqueous solution and the removal efficiency was examined by UV spectroscopy (Fig.9.) The MB consists of base peak at 663 nm which was gradually decreased after every 6 mints when interact with the nanocomposite. Decolorizing efficiency of rGO and bare AgNPs was also investigated. In bare AgNPs, no sudden decolorizing effect was observed. Meanwhile, rGO does not show complete decolorisation. When the

interaction time is increased to 30 mints, decolorization process was completed only in AgNPs-rGO composite which is also confirmed by the color change of the MB dye (fig. 10.). For the adsorption of MB the π–π interaction and electrostatic interaction act as driving forces. MB has rich aromatic rings and cationic atoms. The electrostatic attraction is due to the positively charged functional group of the dye molecule and the negatively charged oxygen containing surface of the rGO. Similarly the enhanced π–π interaction is due to the localized π electrons in the conjugated aromatic rings of the both dye and adsorbent molecules.

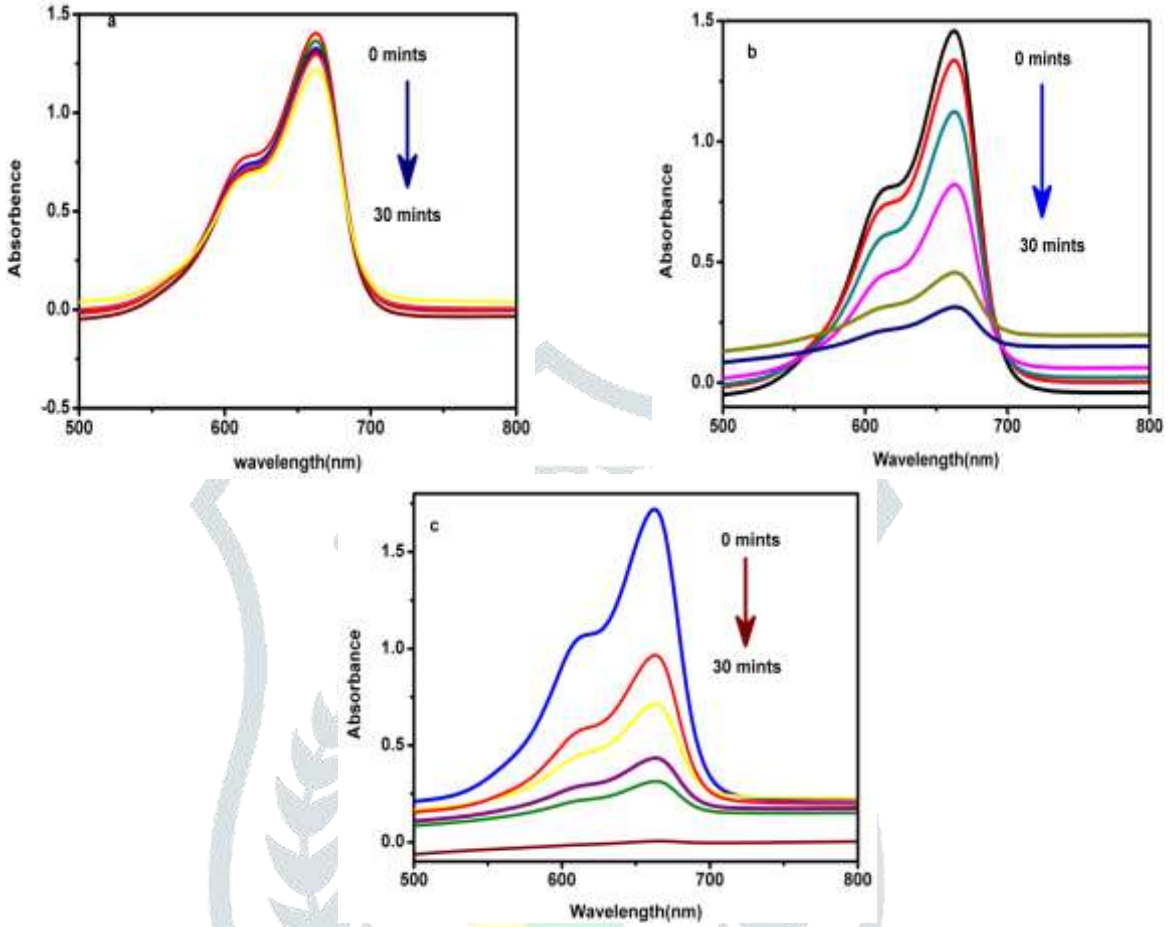

fig.9. uv- vis spectrum of adsorption of MB by using a) rGO b) AgNPs c) AgNPs- rGO

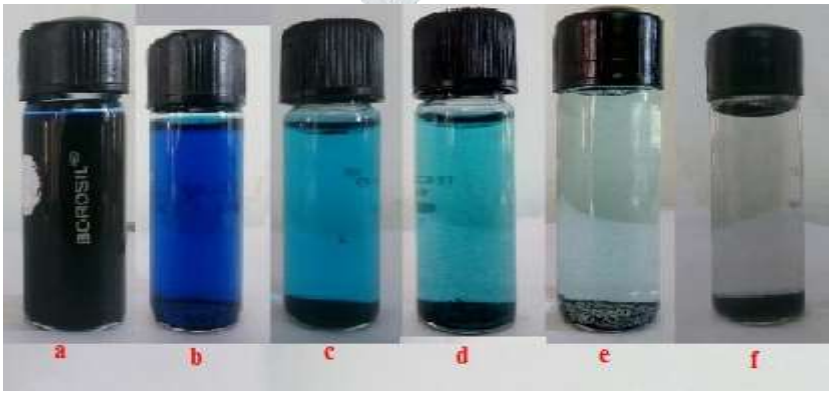

fig.10. photographic images of adsorption of MB by AgNPs- rGO at a) 0 mints b) 6 mints c) 12 mints d) 18 mints e) 24 mints f) 30 mints

The reaction between AgNPs and H_2O or H^+ can produce atom H, which stimulate the destroying the chromophore group and conjugated system of the dye. Schematic illustration of the strategy for the formation of AgNPs-rGO composite and MB degradation mechanism will explained in scheme 1.

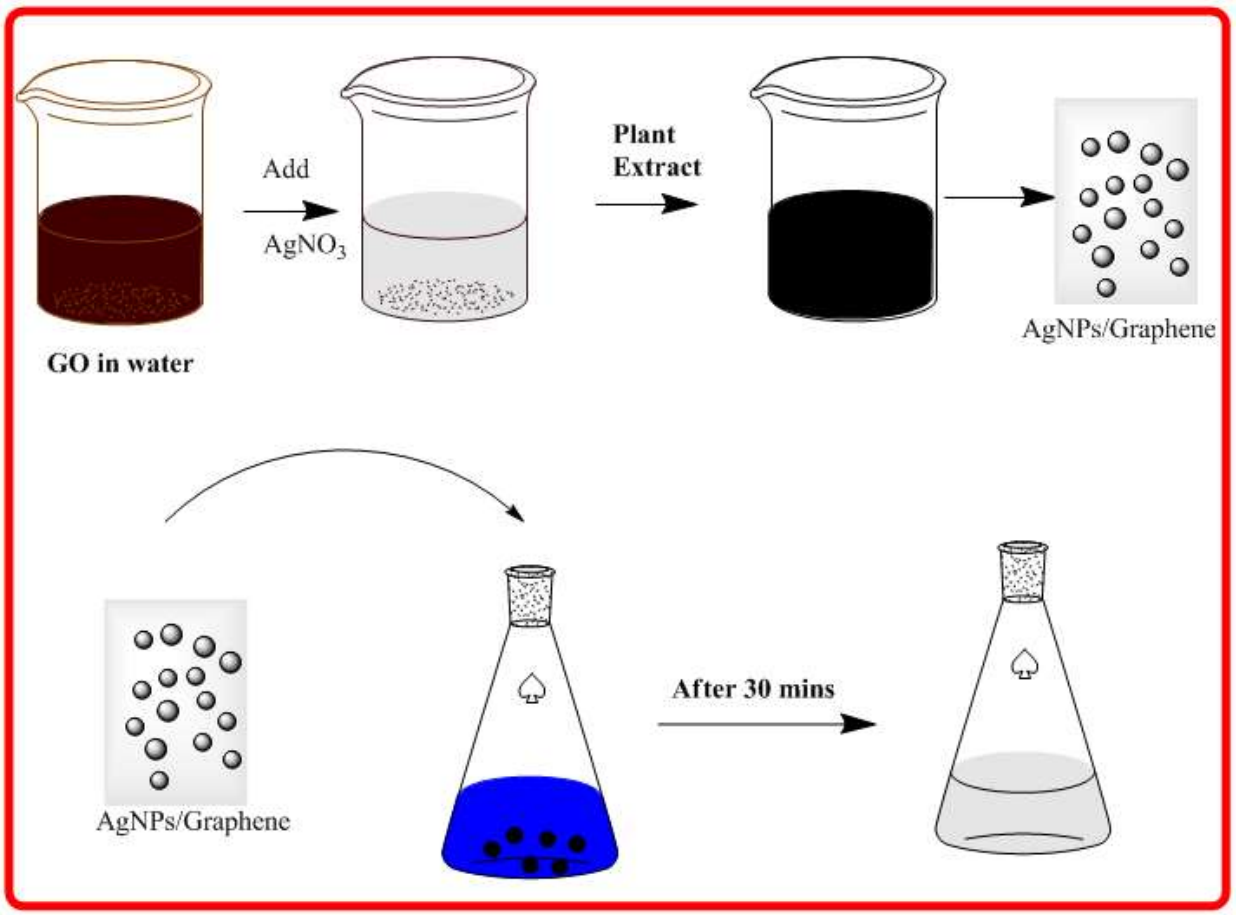

scheme.1.schematic illustration of the strategy for the formation of AgNPs-rGO composite and MB degradation.

The Maximum adsorption capacity and other parameters for adsorption were compared with some previously reported adsorbents that have been used for MB removal and listed in Table 4 [55-66].From this data, we conclude that the adsorption capacity of MB onto AgNPs-rGO composite is higher than that of other reported adsorbents.

table. 4. comparison of adsorption of MB by various adsorbent

Adsorbent	Adsorbent Dosage (mg)	Concentration Of Dye(ppm)	Time (mins)	Adsorption Capacity (mg/g)	Isotherm	Kinetics	Ref
Graphene Oxide	330	100	5	714	Langmuir	Pseudo Second order	55
MNP@St-g-PVS	10	500	120	621	Langmuir	Pseudo Second order	56
MgSi/RGO	20	500	12	433	Langmuir	Pseudo Second order	57

CNTs-A	30	500	90	400	Freundlich	Pseudo Second order	58
3D GO sponge	10	1.2mM (5ml)	2	397	Langmuir	Pseudo Second order	59
GO	10	3	60	350	Langmuir	Pseudo Second order	60
Magnetite/silica/ pectin NPs	2000	100	120	178.57	Langmuir	Pseudo Second order	61
MoS_2 nanosheets	5	20	5	146.43	Freundlich	Pseudo Second order	62
20%GO-Ag-CNF	25	600	10	126.6	Langmui	Pseudo Second order	63
MWCNT	20	20	60	59.7	Freundlich	Pseudo Second order	64
graphene/magnetite composite	10	15	20	43.8	Langmuir	Pseudo Second order	65
Activated Carbon/Cobalt Agrrite/Alginate Composite Beads	70	2.67x 10^{-4} (mol kg^{-1})	120	0.095 (mol kg^{-1})	Langmuir	Pseudo Second order	66
AgNPs-rGO	5	500	30	860.4	Langmuir	Pseudo Second order	**Present work**

Further, SEM images of before and after adsorption of MB by AgNPs, rGO and AgNPs -rGO as shown in Fig 11. SEM images of before adsorption reveals that the rGO sheets decorated uniformly by AgNPs.

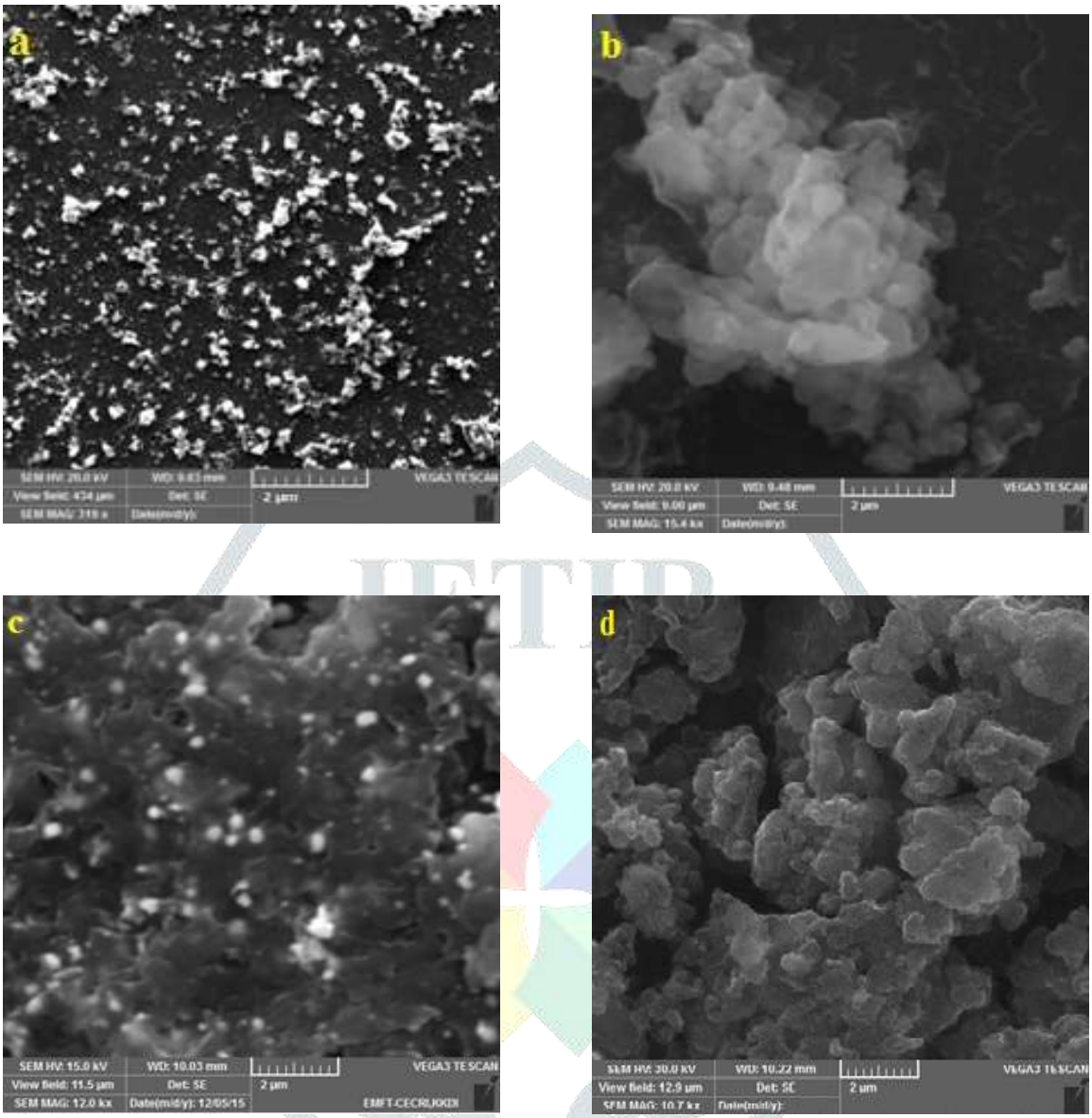

fig.11. sem images of a) AgNPs b) rGO and c) AgNPs-rGO d) AgNPs-rGO after adsorption of MB

After adsorption, it is clearly seen that the size and structure of synthesized materials was changed. There are some cracks and irregularities structure is formed on the surface due to adsorption of MB molecules in the interior portion of the materials.

Reusability

As is well known, an efficient adsorbent should exhibit not only high adsorption capacity but also good stability and reusability in order to reduce the overall cost and also is vital for water treatment application. Thus, the regeneration performance of AgNPs-rGO was analyzed are shown in Fig.12. By comparing the removal efficiency of dyes on the regenerated and fresh adsorbent, it can be concluded that more than 90% of MB can be removed from the solution by the regenerated adsorbent even after five cycles.

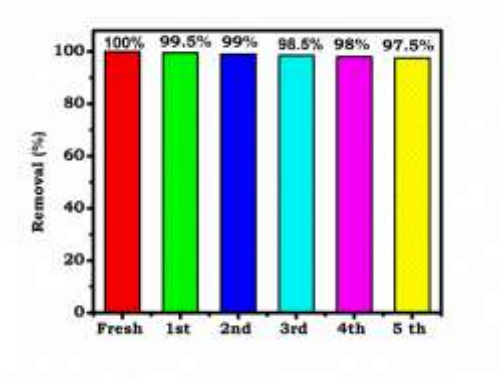

More importantly, desorption of the cationic MB dye was demonstrated simply by washing with deionized water Therefore the AgNPs-rGO can be repeatedly used as a promising adsorbent for removal of cationic dyes from aqueous solution.

Conclusion

In summary, AgNPs-rGO have been successfully synthesized through simple green method which could be used as an effective, non hazards and recyclable adsorbent for water treatment application. The green synthesized AgNPs-rGO reveals superior performance for the fast and effective removal of MB from aqueous solution, with a maximum adsorption capacity of 860.07mg g^{-1} within 30 min at natural pH and room temperature than other adsorbents reported so far. Thus, the AgNPs-rGO nanocomposite can be considered as a very effective adsorbent for removal of dye molecules from wastewater due to the striking Agatures like high adsorption capacities, separation convenience and facile preparation process from nontoxic materials.

REFERENCES

[1] Xiaoyan L, feifeng W, Qinrong Q, Xingpin L. Liren X, Qinghua C. 2012, Mater Lett ; (66): 370-373.

[2] Majid D, Ali KZ, Muhamad MR, Huang NM, Mohammad H. 2012, Mater Lett;(66): 117-120.

[3] Zhang.Y,S.Liu,L.Wang,X.Qin,J.Tian,W.Lu,etal., 2012,Onepot green synthesis of Ag nanoparticles, graphene nano composites and their applications in SERS, H_2O_2, and glucose sensing, RSC Adv.(2),538–545.

[4]. Iliut.M,C.Leordean, V.Canpean, C.M.Teodorescu, S.Astilean, Anewgreen, 2013, ascorbic acid assisted method forver satile synthesis of Au grapheme hybrids as efficient surface-enhanced Raman scattering platforms, J.Mater.Chem.C1 (4094) 4104.

[5] Allen.sM.J., V.C. Tung, R.B. Kaner, 2010, Chem. Rev. (110), 132.

[6]. Y. He, J. Gao, F. Agng, C. Liu, Y. Peng and S. Wang, 2011, Chem. Eng. J.179,818.

[7]. Y. F. Lin and J. L. Chen, 2013, RSC Adv., 3, 15344-15349.

[8]. A.S.Nair and T.Pradeep, (2004) Reactivity of Au and Ag nanoparticles with halocarbons, Applied Nanoscience, 59-63.

[9]. L.Li, F.Liu, X.Jing, P.Ling, A.Li, (2011), Displacement mechanism of binary competitive adsorption for aqueous divalent metal ions onto a novel IDA-chelating resin: Isotherm and kinetic modeling, Water Res. 45 1177 -1188.

[10] Qian Y., S.B. Lu, F.L. Gao, 2011, J. Mater. Sci.(46),3517

[11]. B. Geng, Z.H. Jin, T.L. Li, X.H. Qi, 2009,Preparation of chitosan-stabilized Ag nanoparticles for removal of hexavalent chromium in water, Sci. Total Environ. 07, 4994–5000.

[12] Y.Tian, P.Yin, R.Qu, C.Wang, H.Zheng, Z.Yu, (2010) Removal of transition metal ions from aqueous solutions by adsorption using a novel hybrid material silica gel chemically modified by triethylene tetramino methylene phosphonic acid, Chem. Eng. J. 162 573–579.

[13] Rao, M. M.; Ramana, D. K.; Seshaiah, K.; Wang, M. C.; Chien, S. W. C. 2009, Removal of some metal ions by activated carbon prepared from Phaseolus aureus hulls. J.Hazard. Mater. 166 (2-3), 1006–1013.

[14]. Zhao, J. O.; Liu, L.; Guo, Q. G.; Shi, J. L.; Zhai, G. T.; Song, J. R.Liu, Z. J. 2008,Growth of carbon nanotubes on the surface of carbon fibers.Carbon 46(2), 380–383.

[15]. N. Boujelben, J. Bouzid and Z. Elouear, 2009, J. Hazard. Mater.163, 376–382.

[16]. R. Han, W. Zou, H. Li, Y. Li and J. Shi, 2006, J. Hazard. Mater., 137, 934–942.

[17]. H. Mekatel, S. Amokrane, B. Bellal, M. Trari and D. Nibou, 2012, Chem. Eng. J., 200, 611–618.

[18]. M. Baikousi, A. B. Bourlinos, A. Douvalis, T. Bakas, D. F. Anagnostopoulos, J. Tucek, K. Safarova, R. Zboril and M. A. Karakassides, 2012, Langmuir, 28, 3918–3930.

[19]. W. Liu, J. Zhang, C. Zhang and L. Ren, 2012, Chem. Eng. J., 189, 295–302.

[20]. C. Luo, Z. Tian, B. Yang, L. Zhang and S. Yan, 2013, Chem. Eng. J., 234, 256–265.

[21]. J. Zhu, S. Wei, H. Gu, S. B. Rapole, Q. Wang, Z. Luo, N. Haldolaarachchige, D. P. Young and Z. Guo, 2012, Environ. Sci. Technol., 46, 977–985.

[22]. El Boujaady, H.; El Rhilassi, A.; Bennani-Ziatni, M.; El Hamri, R.; Taitai, A.; Lacout, 2011, J. L. Desalination 275, 10−16.
[23]. Geim, A. K.; Novoselov, K. S. The rise of graphene. 2007, Nat.Mater. 6, 183−191.
[24]. Edwards, R. S.; Coleman, K. S. 2013, Graphene synthesis: relationship to applications., Nanoscale 5, 38−51.
[25]. Novoselov, K. S.; Geim, A. K.; Morozov, S. V.; Jiang, D.; Zhang, Y.; Dubonos, S. V.; Grigorieva, I. V.; Firsov, A. A. 2004, Electric field effect in atomically thin carbon films. Science 306, 666−669.
[26] El Boujaady, H.; El Rhilassi, A.; Bennani-Ziatni, M.; El Hamri, R.; Taitai, A.; Lacout, 2011,J. L. Desalination 275, 10−16.
[27] Yang, S. T.; Chen, S.; Chang, Y.; Cao, A.; Liu, Y.; Wang, H. 2011, Removal of Methylene Blue from Aqueous Solution by Graphene Oxide. J. Colloid Interface Sci. 359, 24−29.
[28] K.G. Bhattacharyya, A. Sharma, 2005,Kinetics and thermodynamics of methylene blue adsorption on Neem (Azadirachta indica) leaf powder, Dyes Pigments. 65, 51–59.
[29]. Rajesh J. Tayade*, Thillai Sivakumar Natarajan and Hari C. BajajInd. 2009, Photocatalytic Degradation of Methylene Blue Dye Using Ultraviolet Light Emitting diodes. Eng.Chem. Res. 48, 10262–10267.
[30]. E. Razo-Flores, M. Luijten, B. A. Donlon, G. Lettinga and J. A. Field, 1997, Environ. Sci.Technol., 31, 2098–2103.
[31]. N. Kongsricharoern and C. Polprasert, 1996, Water Sci. Technol., 34, 109.
[32]. Selcuk, H. Decolorization, 2005, detoxification of textile wastewater by ozonation and coagulation processes. Dyes Pigm. 64, 217–222.
[33]. Buonomenna, M. G.; Gordano, A.; Golemme, G.; Drioli, E. Preparation, 2009, characterization and use of PEEKWC nanofiltration membranes for removal of Azur B dye from aqueous media. React. Funct. Polym. 69, 259–263.
[34]. M. Unlu, H. Yukseler and U. Yetis, 2009, Desalination, 240, 178–185.
[35]. Liu, C. H.; Wu, J. S.; Chiu, H. C.; Suen, S. Y.; Chu, K. H. 2007, Removal of anionic reactive dyes from water using anion exchange membranes as adsorbers. Water Res. 41, 1491–1500.
[36]. Y. C. Zhang, J. Li, M. Zhang and D. D. Dionysiou, 2011, Environ. Sci.Technol., 45, 9324.
[37]. feddal I. et al., 2013, Adsorption capacity of methylene blue, an organic pollutant, by montmorillonite clay, DesalinWater Treat., 1–8
[38] Arami, M.; Yousefi-Limaee, N.; Mahmoodi, N. M.; Salman- Tabrizi, N. 2006,Equilibrium and kinetics studies for the adsorption of direct and acid dyes from aqueous solution by soy meal hull. J. Hazard. Mater. B135, 171–179.
[39]. W.S. Hummers, R.E. Offeman, 1958, Preparation of graphitic oxide, J. Am. Chem. Soc. 80 , 1339.
[40]. Y. Si, E.T. Samulski, 2008, Synthesis of water soluble graphene, Nano Lett. 8, 1679–1682.
[41]. H. Jabeen, V. Chandra, S. Jung, J.W. Lee, K.S. Kim, S. Bin Kim, (2011) Enhanced Cr(VI) removal using iron nanoparticle decorated grapheme, Nanoscale 3 3583–3585.
[42] Langmuir, I. 1916, The constitution and fundamental properties of solids and liquids. J. Am Chem. Soc. 38, 2221–2295.
[43] Freundlich, H. M. F. 1906, Over the adsorption in solution. j. Phys. Chem. 57, 385–471.
[44]. Ai, L.; Li, M.; Li, M. 2011, Adsorption of Methylene Blue from Aqueous Solution with Activated Carbon / Cobalt ferrite/Alginate Composite Beads: Kinetics, Isotherms, and Thermodynamics. J.Chem. Eng. Data 56, 3475−3483.
[45]. S. Lagergren, 1898.About the theory of so-called adsorption of soluble substances, Kungliga Svenska Vetenskapsakademiens, Handlingar 24,
[46]. Ho, Y. S.; McKay, G. 1998, Sorption of dye from aqueous solution by peat. Chem. Eng. J. 70, 115−124.
[47]. fernandes, A. N.; Almedia, C. A. P.; Debacher, N. A.; Sierra, M. D. S. 2010,Isotherm and thermodynamic data of adsorption of methylene blue from aqueous solution onto peat. J. Mol. Struct. 982, 62−65.
[48]. Weber, W. J., Jr.; Morris, J. C. 1963, Kinetics of adsorption on carbon from solution. J. Sanit. Eng. Div. Am. Soc., Civ. Eng. 89, 31−60.
[49]. Wang, X.; Pan, J.; Guan, W.; Dai, J.; Zou, X.; Yan, Y.; Li, C.; Hu, W. 2011, Selective removal of 3-chlorophenol from aqueous solution using surface molecularly imprinted microspheres. J. Chem. Eng. Data 56, 2793–2801.
[50]. Ip, A. W. M.; Barford, J. P.; McKay, G. 2010, A comparative study on the kinetics and mechanisms of removal of Reactive Black 5 by adsorption onto activated carbons and bone char. Chem. Eng. J. 157, 434–442.
[51]. Hameeda, B. H.; El-Khaiary, M. I. 2008, Removal of basic dye from aqueous medium using a novel agricultural waste material: Pumpkin seed hull. J. Hazard. Mater. 155, 601–609.
[52]. Sibel, T.; Ozcan, A. S.; Ozcan, A.; Gedikbey, T. 2006, Kinetics and equilibrium studies for the adsorption of Acid Red 57 from aqueous solutions onto calcined-alunite. J. Hazard Mater. 135, 141−148.
[53]. Weng, C. H.; Lin, Y. T.; Tzeng, T. W. 2009, Removal of methylene blue from aqueous solution by adsorption onto pineapple leaf powder. J. Hazard. Mater. 170, 417−424.
[54]. fernandes, A. N.; Almedia, C. A. P.; Debacher, N. A.; Sierra, M. D. S. 2010, Isotherm and thermodynamic data of adsorption of methylene blue from aqueous solution onto peat. J. Mol. Struct. 982, 62−65.
[55]. Wenjie Zhang, Chunjiao Zhou, Weichang Zhou, Aihua Lei, Qinglin Zhang, Qiang Wan, Bingsuo Zou,2011, Fast and Considerable Adsorption of Methylene Blue Dye onto Graphene Oxide , Bull Environ Contam Toxicol 87, 86–90
[56]. A. Pourjavadi, A. Abedin Moghanaki and A. Tavakoli. 2016, Efficient removal of cationic dyes using a new magnetic nanocomposite based on starch-g-poly (vinylalcohol) and functionalized with sulfate groups, RSC Adv., DOI: 10.1039/C6RA02517J.
[57]. Chen-Xi Gui, Qian-Qian Wang, Shu-Meng Hao, Jin Qu, Pei-Pei Huang, Chang- Yan Cao, Wei-Guo Song and Zhong-ZhenYu Sandwichlike 2014, Magnesium Silicate/Reduced Graphene Oxide Nanocomposite for Enhanced Pb2+ and Methylene Blue Adsorption , ACS Appl. Mater. Interfaces 6, 14653−14659

[58]. Jie Ma, fei Yu, Lu Zhou, Lu Jin, Mingxuan Yang, Jingshuai Luan, Yuhang Tang, Haibo Fan, Zhiwen Yuan and Junhong Chen, 2012, Enhanced Adsorptive Removal of Methyl Orange and Methylene Blue from Aqueous Solution by Alkali-Activated Multiwalled Carbon Nanotubes. ACS Appl. Mater. Interfaces 4, 5749−5760

[59]. fei Liu, Soyi Chung, Gahee Oh, and Tae Seok Seo. 2012, Three-Dimensional Graphene Oxide Nanostructure for Fast and Efficient Water-Soluble Dye Removal, ACS Appl. Mater. Interfaces, 4, 922−927

[60]. Philip Bradder, Sie King Ling, Shaobin Wang and Shaomin Liu, 2011, Dye Adsorption on Layered Graphite Oxide. J. Chem. Eng. Data 56, 138–141

[61] Olivia A. Attallah, Medhat A. Al-Ghobashy, Marianne Nebsen and Maissa Y. Salemb, 2016, Removal of cationic and anionic dyes from aqueous solution with magnetite/pectin and magnetite/ silica/pectin hybrid nanocomposites: kinetic, isotherm and mechanism analysis, RSC Adv., 6, 11461–11480

[62]. Tian, D. Hou and D. Li, 2016, Equilibrium and kinetic studies on MB adsorption by ultrathin 2D MoS2 nanosheets. RSC Adv., DOI: 10.1039/C5RA24328A.

[63]. Lunhong Aia,b, Chunying Zhangb, Zhonglan Chena,b. 2011,Removal of methylene blue from aqueous solution by a solvothermal-synthesized graphene/magnetite composite. Journal of Hazardous Materials 192, 1515– 1524

[64]. Shaobin Wanga, Choon Wei Ng , Wentai Wangb, Qin Li, Zhengping Hao. 2012, Synergistic and competitive adsorption of organic dyes on multiwalled carbon nanotubes. Chemical Engineering Journal 197, 34–40

[65] M. S. Sajab, C. H. Chia, C. H. Chan, S. Zakaria, H. Kaco, S. W. Chook, S. X. Chin and A.Mohamed Noor, 2016, Bifunctional graphene oxide-cellulose nanofibril aerogel loaded with Ag(III) for removal of cationic dye via simultaneous adsorption and Agnton oxidation. RSC Adv., DOI: 10.1039/C5RA26193G.

[66]. Lunhong Ai, Ming Li and Long Li. 2011,Adsorption of Methylene Blue from Aqueous Solution with Activated Carbon/Cobalt ferrite/Alginate Composite Beads: Kinetics, Isotherms, and Thermodynamics. J. Chem.Eng. Data 56, 3475–3483.